Composites Part C: Open Access 15 (2024) 100538

Contents lists available at ScienceDirect

Composites Part C: Open Access

journal homepage: www.sciencedirect.com/journal/composites-part-c-open-access

Plastic deformation assessment of sawdust-rPET composites under bending load

S. Behnam Hosseini [a], Milan Gaff [a,b,*], Jerzy Smardzewski [c]

[a] Department of Furniture, Design and Habitat Brno, Mendel University in Brno 61300, Brno, Czech Republic
[b] Faculty of Civil Engineering, Experimental Centre, Czech Technical University in Prague, Thakurova 7, 166 29 Prague 6, Czech Republic
[c] Department of Furniture Design, Faculty of Forestry and Wood Technology, Poznan University of Life Science, ul. Wojska Polskiego 28 60-637, Poznan, Poland

ARTICLE INFO

Key words:
Sawdust
Waste PET
Polymer composite
Mechanical properties
Bending properties

ABSTRACT

Due to the scarcity of raw wood materials and the current state of the market's economic growth, the development of novel composite materials utilizing alternate raw material sources is crucial. Sawdust and waste polymers, such as empty bottles, are excellent sources of low-cost materials for making useful and cost-effective wood-plastic composites. This article's main goal is to ascertain how different filler contents and percentages, as well as two different types of polymer matrices, affect the mechanical properties of sawdust-reinforced composite in the plastic range of force-deflection diagram of bending test. Sawdust-plastic composites based on waste polyethylene terephthalate (PET) and biodegradable polymers were produced by the flat press method and prepared for mechanical testing. This study examined comprehensively the plastic range of the three-point bending test. The limit of proportionality (LOP), bending strength or modulus of rupture (MOR), plastic potential "P_P", four tangent moduli as well as approximated plastic work "A_W", total plastic work "B_W" and the values of approximation error "ΔW" were measured using three-point bending test. The finite element method (FEM) analysis was also conducted to prepare a numerical model and compare its results with experimental results. According to the study's findings, the bending features of rPET-reinforced composites declined as the filler percentage increased. Among all the rPET-reinforced composites, the 40 % sawdust filled composite had the best mechanical performance. When compared to the rPET matrix, the biodegradable polymer demonstrated superior mechanical performance in the plastic zone of the bending test. However, both the 40 % sawdust-filled rPET composite and the biodegradable composites filled with 50 % sawdust fulfilled the ANSI standard as an appropriate replacement for medium-density fiberboard (MDF) for interior applications.

1. Introduction

A manufactured composite called wood plastic composite (WPC) is created by embedding wood fiber or flour into a polymer matrix. The two major types of polymers are thermoplastic and thermoset. The majority of the thermoplastic polymers utilized as a polymer matrix for wood particles are polypropylene (PP), polyvinyl chloride (PVC), and high-density polyethylene (HDPE), while the most frequently applied thermoset polymers for wood composites are epoxy, polyester, resins, and phenolic [1]. The most popular thermoplastic polymers utilized in wood-plastic composites are PP, HDPE, and PVC because they can be drilled, screwed, pinned down, and trimmed with instruments that have previously been employed for woodworking, and their manufacturing temperatures are frequently less than 180–200 °C (the wood degradation temperature) [2]. Because wood is an organic resource, WPCs are relatively environmentally friendly, reducing waste and protecting the environment. Even though most polymers are not biodegradable, the non-biodegradable fraction of wood plastic composites is greatly decreased when wood fibers and other lignocellulosic-based materials, such as agriculture waste, are mixed into polymers up to 40–70 wt%. [3]. Moreover, waste polymers are useable to create wood-plastic composites with the least amount of environmental impact. Lastly, the wood fiber as well as thermoplastic polymer characteristics of wood plastic composites make them easier to decompose and recycle. Furthermore, the usage of biodegradable polymers such as polylactic acid (PLA) has been growing in recent years in the wood plastic composite industry, allowing for the producing of completely biodegradable composites that are environmentally friendly and

* Corresponding author.
E-mail address: gaffmilan@gmail.com (M. Gaff).

https://doi.org/10.1016/j.jcomc.2024.100538

Available online 22 November 2024

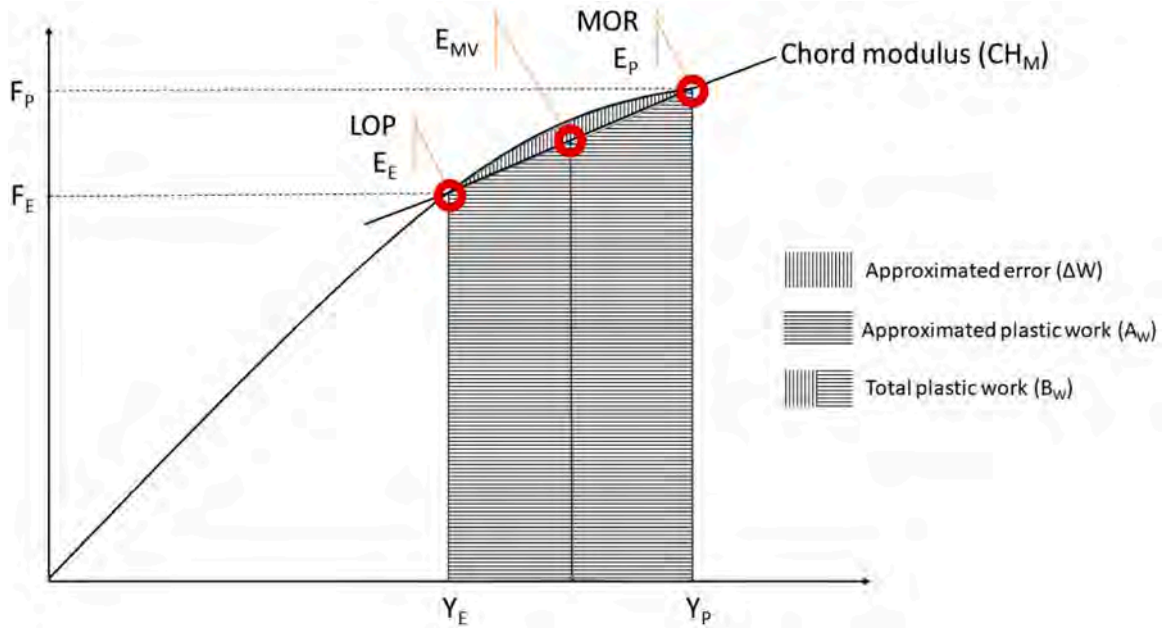

Fig. 1. The bending properties in the plastic range of force-deflection's diagram.

Table 1
The composition of composites.

Composite Code	Composition
S4P6	Sawdust (40 %), PET waste (60 %)
S6P4	Sawdust (60 %), PET waste (40 %)
S5Y5	Sawdust (50 %), Y1000P polymer (50 %)
S2R4P4	Sawdust (20 %), Rubber (40 %), PET waste (40 %)

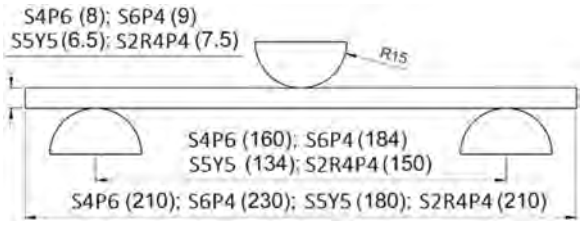

Fig. 2. Bending test and sample properties (sample dimensions were presented in the parenthesis in mm).

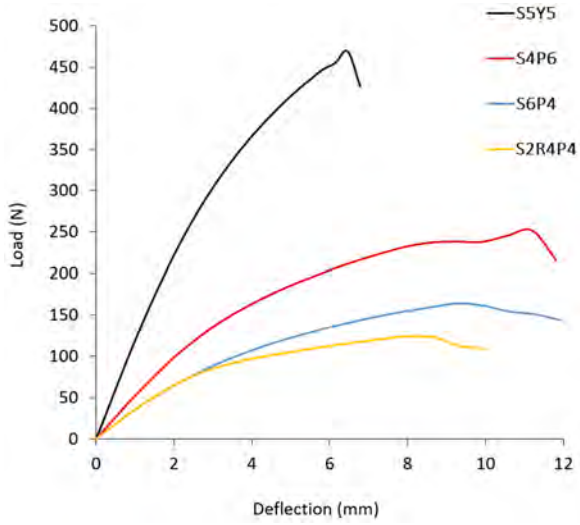

Fig. 3. Load-deflection relation for experimental tests.

decrease ecological concerns about plastic usage [4].

The popularity of lignocellulosic materials as low-cost, eco-friendly substitutes for wood particles in plastic composites was prompted by rising wood prices and competition for available wood resources [5]. These materials can be wood (sawdust or waste wood particles) or non-wood (agricultural waste) and are primarily used in outdoor uses including playground equipment, door frames, windows, fencing, decking, etc. [6]. Sawdust is an inexpensive, easily accessible, and light-weight material which might be utilized in composite materials [4]. Recent studies indicate that extensive research has been done on natural fibers in order to create bio-composites [5–18]. By incorporating natural fibers into a polymer matrix, the mechanical characteristics of composites can typically be dramatically improved, as fibers possess far higher quantities of strength and stiffness than polymers [4].

Due to composite bending takes place in practically all of its service situations, bending properties are the most frequently evaluated mechanical properties of wood-based composite materials. It usually arises when furniture products or construction components are being loaded [19]. Hence, the flexural properties of WPCs under bending loads turn out to be one of the main mechanical characteristics of WPC-based products, and it has been investigated using analyzing force-deflection results of WPCs. A force-deflection diagram allows us to understand how materials behave when they are under mechanical forces and the diagram provides the determination of numerous mechanical parameters. Fig. 1 shows a common strain-strain diagram [20].

The diagram is divided into two sections, where the first part is based on Hooke's law and there is a straight-line connection between force and deflection and the tangent modulus is described as the modulus of elasticity (MOE) [20]. The proportionality limit is the final point in the liner segment. Plastic and viscoelastic deformations take place when the stress exceeds the limit of proportionality, and hereafter, the "plastic region" term will be used for simplicity. As the force-deflection diagram in the plastic zone is not linear, there are various tangent models that can be described by the slope of the force-deflection curve at any given point [20]. There are many authors referred to modulus in the plastic range which can be found in other studies, e.g. Požgaj et al. [21] defines the modulus of plasticity as the relationship between force and

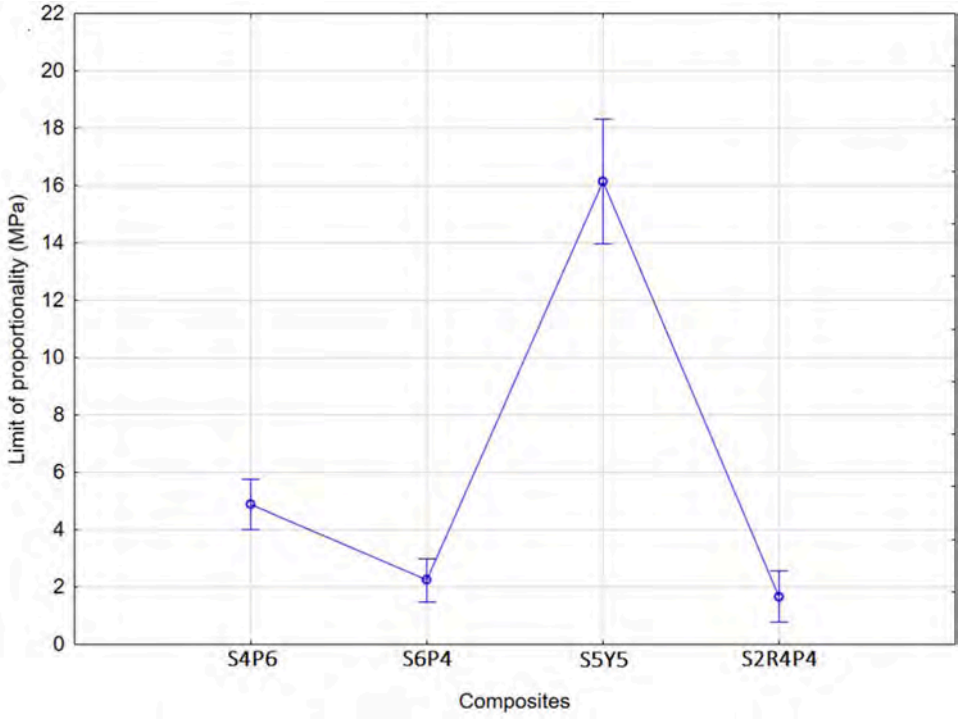

Fig. 4. The effect of different compositions on the proportionality limit of composites.

Table 2
The Duncan's test results of the proportionality limit of reinforced composites as function of different composition.

Composites		(1) 4.8728	(2) 2.2372	(3) 16,148	(4) 1.6622
1	S4P6		0.002831	0.000121	0.000588
2	S6P4	0.002831		0.000063	0.486879
3	S5Y5	0.000121	0.000063		0.000053
4	S2R4P4	0.000588	0.486879	0.000053	

deflection at a specific spot on the curve from the proportionality limit to modulus of rupture (MOR). Terms like tangent modulus and secant modulus are employed by other authors frequently for plastic deformation of solid materials (like metal), but not usually for wood-based products [22].

The majority of studies focus on limit of proportionality, Young's modulus in the elastic range, and bending strength (modulus of rupture) of stress-strain's diagram, whereas there are a lot of mechanical characteristics on bending diagram especially in the plastic region. The aim of this study was to determine the effect of different compositions on the bending properties of composite material in the plastic range including the limit of proportionality (LOP), the Chord modulus (CH_M), the tangent modulus at the elasticity point (E_E), the middle point's tangent modulus (E_{MV}), the MOR point's tangent modulus (E_P), approximated plastic work (A_W), total plastic work (B_W) and the values of approximation error (ΔW) as well as investigation of numerical modeling of produced composited using finite element method (FEM).

2. Materials and methods

2.1. Materials

Sawdust was sieved to a particle size of 0.5 mm and taken from the local workshop at Mendel University in Brno. The rubber filler was prepared by sieving waste tires to under 0.2 mm. The prepared sawdust and rubber particles dried in an oven at 103 ± 2 °C for 24 h to reach moisture content of 2 %. To obtain recycled PET powder, used drinking water bottles have been collected locally and ground in a grinder. Oversized particles were eliminated from the PET powder by sieving it through a 60 mesh screen. The PET powder was also dried for 24 h at 103 ± 2 °C in an oven to reduce its moisture content to 2 %. For recycled PET, the corresponding values for density, melt flow index, and melting point were 1370 Kg/m^3, 18.4 g/10 min, and 260 °C, respectively [23].

Poly [(3-hydroxybutyrate)-co-(3-hydroxyvalerate)] (PHBV) under trade name of Enmat Y1000P, was purchased from Ningbo Tianan Biologic Material (Ningbo, China). In addition to being aligned with EU REACH Regulation EC 1907/2006, Y1000P is also mentioned in EU Commission Regulation No. 10/2011 (Annex I, Table 1, no. 744). The molecular weight (Mw) of the Y1000P biopolymer is approximately 280.000 g.mol^{-1}, its melting temperature (T_m) is 176 °C, its valeric acid content is approximately 3 mol %, and its density is 1250 kg/m^3 [24, 25].

2.2. Sample preparation

To create uniform wood-plastic composites, the sawdust and polymer were combined in a rotating drum blender using the ratio shown in Table 1. WPC panels were produced utilizing a laboratory press (Strozatech, Czech Republic) and a flat press method. The mixture was placed in a 39 × 39 × 0.5 cm metal frame to produce a homogenous mat. The press cycle could be separated into three stages [26]: the first stage involved manually pressing the mat to lower its height; the second stage involved moving it to an improvised hot press that was heated by electricity to press it hot; and the final stage involved using a cold press to cool the WPC panels to room temperature while maintaining a constant panel thickness [27]. The press pressure, maximum pressing temperature, hot and cold pressing time were 5 N/mm^2, 190 °C, 5 and 6 min, respectively. The temperature was lowered (190 °C) from the PET's melting point of 260 °C in order to prevent the wood's degeneration [23]. For each composite, three replications were produced, which were then cut into test samples and subjected to a standardized equilibrium moisture content (EMC) in climate chamber HCP 108 (Memmert, Germany) for two days at ϕ=65 ± 1 % and t = 20 ± 1 °C.

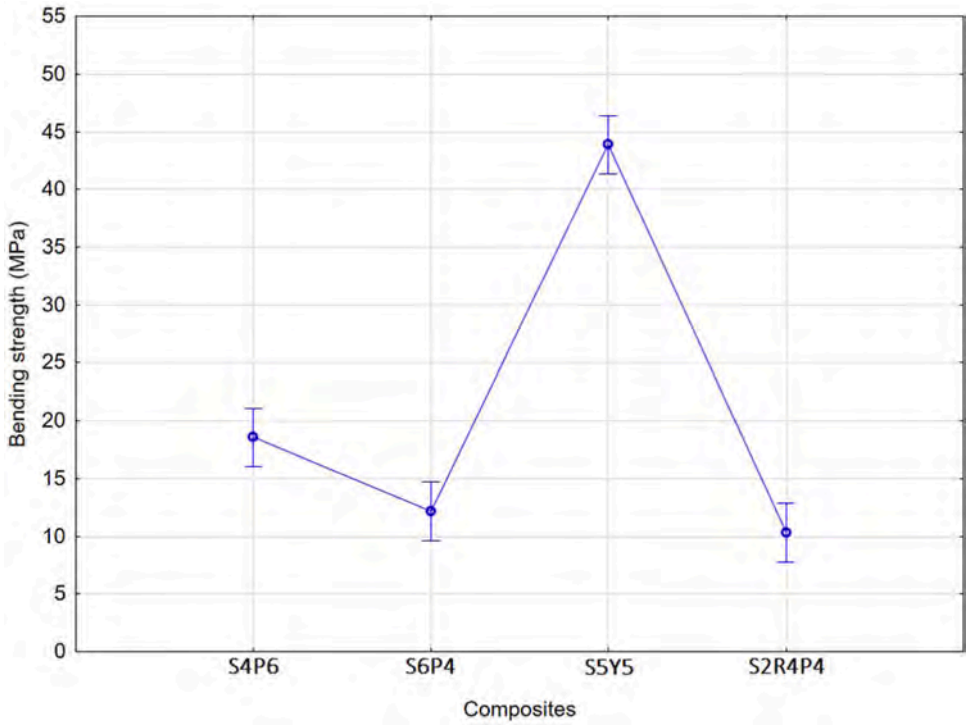

Fig. 5. The effect of different compositions on the composites' bending strength.

Table 3
The Duncan's test results of the bending strength of reinforced composites as function of different composition.

Composites		(1) 18.584	(2) 12.159	(3) 43.877	(4) 13.321
1	S4P6		0.000970	0.000121	0.000114
2	S6P4	0.000970		0.000063	0.304409
3	S5Y5	0.000121	0.000063		0.000053
4	S2R4P4	0.000114	0.304409	0.000053	

2.3. Mechanical properties

The specimens were bent by 3-point bending test using a universal testing machine ZWICK Z050 (Ulm, Germany) according to ISO 13,061–3 with loading speed of 10 mm/min (Fig. 2). The support length was set according to the specimens' thickness (h) multiplied by 20 ($l = 20 \times h$).

The evaluated force-deformation diagram provided the values for all the properties that were examined, including bending strength and various modules [22,27].

The point at which the curve deviates more than 1 % from the linear portion (Fig. 1) is known as the limit of proportionality, or LOP [22] based on Eq. (1) and EN 310 standard.

$$LOP = \frac{3F_E l_0}{2bh^2} \tag{1}$$

where LOP is the limit of proportionality (MPa), F_E is the force at the limit of proportionality (N), l_0 is the support span (mm), b is the width of the sample (mm), and h is the height (thickness) of the sample (mm).

The bending strength or modulus of rupture (MOR) was obtained according to ISO 13,061–3 and Eq. (2),

$$\sigma_B = \frac{3F_{max} l_0}{2bh^2} \tag{2}$$

where σB is the bending strength (MPa), F_{max} is the force at the maximum bending strength (N), l_0 is the distance between the centers of the supports (mm), b is the width of the specimen (mm), and h is the thickness of the specimen (mm).

The deflection's plastic work could be calculated using the integration of the regression Eq. (3) of the plastic area trend of the force-deflection diagram (Fig. 1).

$$F(x) = ax^2 + bx + c \tag{3}$$

The plastic work (eq. (5)) was obtained by integrating this equation within the limits Y_E and Y_P (eq. (4)):

$$B_W = \int_{Y_E}^{Y_P} F(x)dx = \int_{Y_E}^{Y_P} (ax^2 + bx + c)dx \tag{4}$$

$$B_W = \frac{a}{3}\left[Y_P^3 - Y_E^3\right] + \frac{b}{2}\left[Y_P^2 - Y_E^2\right] + C[Y_P - Y_E] \tag{5}$$

The suggested work definition has some complexity because it needs to calculate coefficients a, b, and c. The linear approximation (Fig. 1) utilizing the chord modulus between the strength limit "F_P" and the proportionality limit "F_E" is an easiest approach. Eq. (6) is used to calculate the approximate plastic work (A_W).

$$A_w = \frac{F_P + F_E}{2}(Y_P - Y_E) \tag{6}$$

where F_P is the force at the strength limit (N), F_E is the force at the proportionality limit (N), Y_P is the deflection at the strength limit (mm), and Y_E is the deflection at the limit of proportionality (mm).

The approximation error (Fig. 1) is the difference between the estimated values and the real values of the work, which can be expressed as a percentage using Eq. (7).

$$W = B_W - A_W \tag{7}$$

The plastic potential can be calculated by dividing the work of deformation in the plastic range by the volume of the sample within the stressed area, based on Eq. (8):

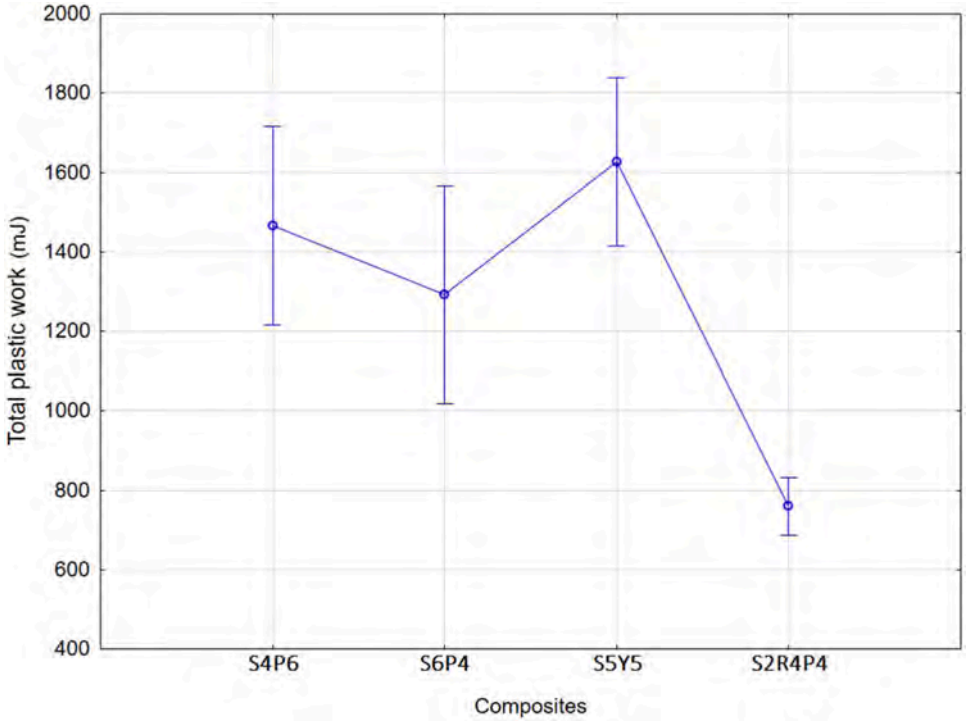

Fig. 6. The effect of different compositions on total plastic work of composites.

Table 4
The Duncan's test results of the total plastic work of reinforced composites as function of different composition.

Composites		(1) 1465.7	(2) 1292.9	(3) 1627.6	(4) 759.78
1	S4P6		0.210416	0.240373	0.000073
2	S6P4	0.210416		0.023960	0.000474
3	S5Y5	0.240373	0.023960		0.000053
4	S2R4P4	0.000073	0.000474	0.000053	

$$P_P = \frac{B_W}{bhl_0} \tag{8}$$

where P_P is the plastic potential (MPa), B_w is the viscoplastic range's deformation work (mJ), b is the specimen's width (mm), h is the specimen's thickness of the (mm) and l_0 is the support span (mm). Y_P is the deflection at the modulus of rupture (mm), Y_E is the deflection at the limit of proportionality (mm).

The initial derivative of the force-displacement or stress-strain diagram is known as the tangent modulus. The current study utilized derivations from Babiak and Gaff [20] to calculate different modules:

The tangent modulus at the elasticity point "E_E"

$$E_E = \frac{F_E}{Y_E} \times \frac{l_0^3}{48I} \tag{9}$$

The middle point's tangent modulus "E_{MV}"

$$E_{MV} = \frac{F_{MV}}{Y_{MV}} \times \frac{l_0^3}{48I} \tag{10}$$

The MOR point's tangent modulus "E_P"

$$E_P = \frac{F_P}{Y_P} \times \frac{l_0^3}{48I} \tag{11}$$

The chord modulus of three-point bending was calculated using the following Eq. (12):

$$CH_M = \frac{F_P - F_E}{Y_P - Y_E} \times \frac{l_0^3}{4bh^3} \tag{12}$$

where F_P is the maximum force at the plastic range (N), F_E is the force at LOP (N), Y_P is the deflection at the strength limit (mm), and Y_E is the proportionality limit (mm), F_{MV} is the force at middle value (N) according to $F_{MV} = (F_E + F_P)/2$, Y_{MV} is the deflection at middle value (mm) according to $Y_{MV} = (Y_E + Y_P)/2$, I is the moment of inertia according to $I = bh^3/12$, b is the specimen's width (mm), h is the specimen's thickness (mm) and l_0 is the support span (mm).

2.4. Statistical analysis

Using Duncan's tests and STATISTICA software, the effects of each individual item on the bending properties were assessed using an ANOVA analysis with a 95 % confidence interval that represents a significance level of 0.05 ($P < 0.05$), and Duncan grouping test was used to confirm the findings of the study. All statistical analyses conducted by STATISTICA software (version 14, Statsoft Inc., USA).

3. Results of experimental tests

Fig. 3 depicted force-deflection results of investigated reinforced composites. According to Fig. 3, the biodegradable composite containing 50 % sawdust showed the highest mechanical performance in all (elastic and plastic) zones followed by rPET reinforced composites with noticeable lower force endurance.

Fig. 4 and table 2 represent the limit of proportionality (LOP) of reinforced composites as well as Duncan grouping results, respectively. The biodegradable polymer composite containing 50 % sawdust demonstrated the highest limit of proportionality (4.872 MPa). The rPET-reinforced composites demonstrated lower amounts of the limit of proportionality, where the lowest LOP (1.662 MPa) belongs to rPET composite containing mixed sawdust-rubber filler. Based on the Duncan grouping test (Table 2), there is no significant difference between reinforced composites containing 60 % filler neither 60 % sawdust nor

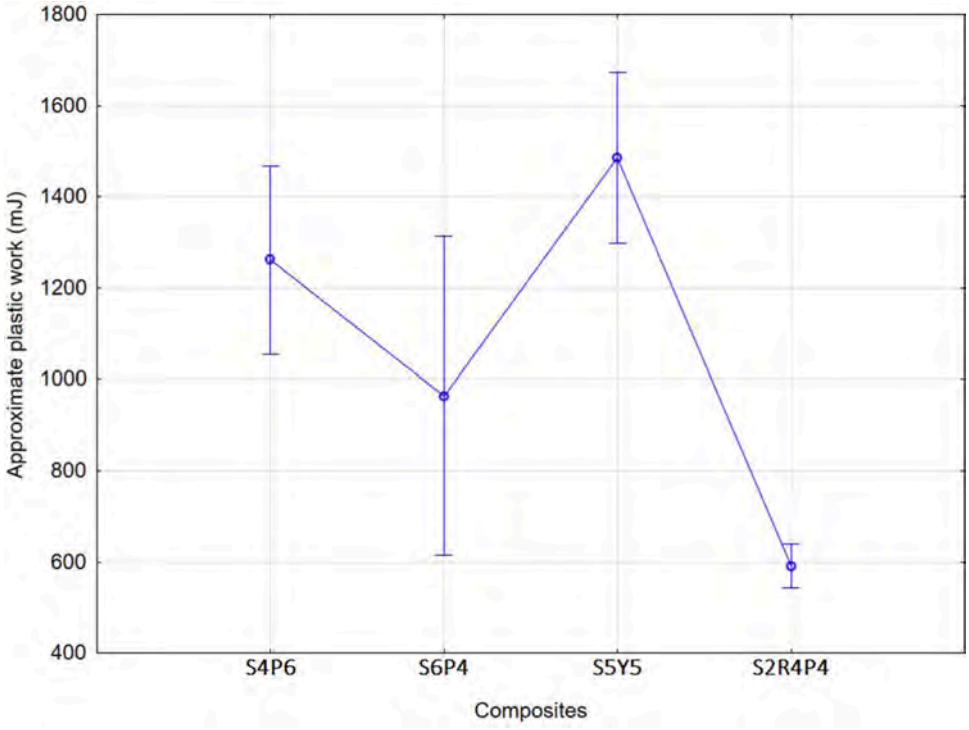

Fig. 7. The effect of different compositions on approximate plastic work of composites.

Table 5
The Duncan's test results of the approximate plastic work of reinforced composites as function of different composition.

Composites		(1) 1261.7	(2) 963.73	(3) 1484.8	(4) 591.07
1	S4P6		0.040871	0.121087	0.000101
2	S6P4	0.040871		0.001030	0.011890
3	S5Y5	0.121087	0.001030		0.000053
4	S2R4P4	0.000101	0.011890	0.000053	

20 % sawdust+40 % rubber. According to Fig. 4 and Duncan grouping test (Table 2), the rPET composite containing lower amount of filler (40 %) showed higher mechanical performance (4.872 MPa) with significant difference compared to 60 % filled rPET-composites. Unappropriated covering of sawdust particles with polymer matrix in 60 % or more sawdust ratio could be the reason of the LOP's decreasing [28]. However, there was a magnificent increase in LOP by replacing rPET matrix with biodegradable which is the most important factor compared to filler percentage and composition.

The composites' bending strength were depicted in Fig. 5. The results of bending strength or modulus of rupture (MOR) and Duncan grouping test (Table 3) demonstrated as same trend as limit of proportionality, where biodegradable composite containing 50 % sawdust and 40 % filled rPET-composite showed the higher bending strength values (43.877 and 18.583 MPa), respectively. The reinforced composites containing 60 % sawdust and mixed natural fiber and rubber particles showed minimum bending strength of 12.159 and 10.320 MPa without significant difference, respectively (Table 3). As it was verified by the Duncan test (Table 3), there was a significant difference between 40 and 60 % filler filled composites. According to Fig. 5, the best bending strength performance among rPET reinforced composites belongs to 40 % sawdust composite (18.583 MPa), where a lower amount of natural filler led to an increase in the mechanical properties of composites significantly. The uniform distribution of the lignocellulosic components scattered within the polymer material could decrease by increasing the sawdust content and led to gradually reduction of the rPET matrix's binding capacity [26,29].

The decrease of MOR with increasing sawdust amount is confirmed with findings from many studies [23,30,31]. According to Klímek et al. [32], increasing the amount of plasma-treated PET flakes from 15 to 30 % decreased MOR values of particleboards. However, only module of rupture of the 40 % sawdust rPET and 50 % sawdust biodegradable composites met requirements of ANSI standards (14 N/mm^2) for the medium density fiberboard (MDF).

The results of total plastic work of investigated bio-composites were depicted in Fig. 6. The findings indicated that the biodegradable reinforced composites containing 50 % sawdust showed maximum total plastic work (1627.587 mJ) and followed by rPET composite with 40 % sawdust (1465.741 mJ). According to the Fig. 6, the 60 % filled composites showed noticeable difference results, where 60 % sawdust reached to 1292.862 mJ whereas 60 % mixed filler (sawdust-rubber) demonstrated the lowest total plastic work (759.776 mJ) among all composites. General, the addition of rubber particles led to a decrease in total plastic work substantially. It could be attributed to the higher size of rubber particles compared to sawdust which reduce uniform distribution of force within composites under bending load as well as different nature of rubber particles compared to natural fibers. According to Maloney [33], a possible additional factor contributing to the mechanical loss of the composites could be the fine materials' relatively large surface area. The Duncan test also confirmed that reinforced composites made with mixed fillers of rubber and sawdust had a significant difference in total plastic work in comparison to natural fiber-reinforced composites (Table 4).

Approximate plastic work of reinforced composites as the area under chord modulus line in plastic range of force-deflection diagram was presented in Fig. 7. The maximum and minimum approximate plastic work belong to biodegradable composite containing 50 % natural fiber and 60 % mixed filer filled composite with values of 1484.778 and 591.070 mJ, respectively. As it is obvious from Fig. 7, increasing filler into rPET matrix led to lower amounts of approximate plastic work, where the 40 % filled rPET-composite with sawdust showed the highest

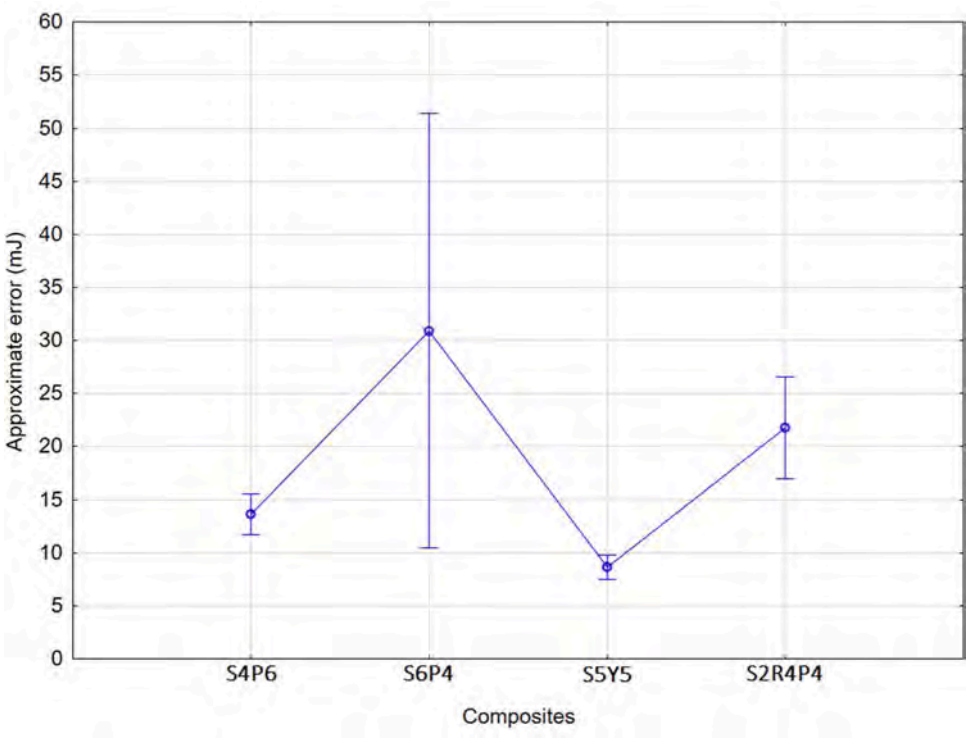

Fig. 8. The effect of different compositions on approximate error of composites.

Table 6
The Duncan's test results of the approximate error of reinforced composites as function of different composition.

Composites		(1) 13,596	(2) 30,902	(3) 8.6574	(4) 21,772
1	S4P6		0.017058	0.460319	0.224508
2	S6P4	0.017058		0.003216	0.176163
3	S5Y5	0.460319	0.003216		0.067896
4	S2R4P4	0.224508	0.176163	0.067896	

approximate plastic work (1261.739 mJ) among all rPET composites. Because of sawdust's incompatibility with polymeric matrix, non-uniform distribution, weak fiber-matrix bonding, and stress concentration effects at its corners, it is known to decrease the mechanical properties of WPCs [34]. The findings of the Duncan grouping test indicated significant difference of approximate plastic work between all investigated composites except biodegradable polymer composite with 50 % sawdust and rPET composites containing 40 % sawdust (Table 5).

According to definition, the approximate error is difference between total plastic work and approximate plastic work (Fig. 1). The results of approximate error were depicted in Fig. 8, where biodegradable reinforced composite containing 50 % sawdust showed minimum approximate error (8.657 mJ). The 60 % sawdust and mixed sawdust-rubber composites reached higher values of approximate error of 30.901 and 21.772 mJ, respectively. According to Fig. 8, the filled composites with lower amounts of fillers (40–50 %) reached to minimum approximate error compared to higher filler ratio composites (60 %). Duncan grouping test of approximate error revealed only two significant differences with confidence level of 95 % among all investigated composites (Table 6). The first one occurred between biodegradable reinforced composite by 50 % sawdust and rPET composite with 60 % sawdust. The second one was observed between rPET composites filled with 40 and 60 % sawdust (Table 6).

The outcomes of the bending test of composites showed that plasticity potential of composites decreased by increasing the plastic to filler ratio (Fig. 9). Biodegradable reinforced polymer containing 50 % sawdust showed the higher plasticity potential (0.027 MPa). By contrast, rPET composite containing higher ratio of polymer showed better performance in the evaluated mechanical property (0.017 MPa) which might be explained by a greater density of PET compared to sawdust [23] and subsequently led to increase the mechanical features of composites. The Duncan grouping test also revealed that a higher polymer ratio led to a significant difference in plasticity potential compared to lower polymer content composites (Table 7).

The results of four bending modules in the plastic range of force-deflation bending diagram including E_E, E_{MV}, E_P, and CH_M as well as Duncan grouping test were presented in tables 8 and 9, respectively. All evaluated modules showed same trend, where the composite containing biodegradable polymer showed highest values in all bending modules with maximum value of 4877 MPa at the proportionality Limit (E_E). The bending modules in plastic range reduced as filler amount increased, where both rPET reinforced composites containing 60 % sawdust and mixed sawdust/rubber (20/40 % ratio) showed no significant difference (Table 9). By contrast, 40 % sawdust composite demonstrated significant difference and also higher modules compared to other rPET composites with maximum value of 1961 MPa at the proportionality limit (E_E) (Table 8). In other words, lower amounts of fillers led to better module results for all investigated rPET composites.

The poorer sawdust-rPET interfacial contact may be the cause of the lower modules with increased sawdust content. Due to the pressing temperature was only 190 °C and the melting point of rPET was 260 °C, the polymer matrix may not flow easily inside the composites [23]. The performance of the rPET WPCs could be improved by the addition of additives such coupling agents [35]. It is reported by many researchers that the addition of coupling agents to the compositions led to better polymer-filler interaction [36–39] and also decreased the melting point of PET [23], resulting in better mechanical properties.

Fig. 10 shows the maximum force at the strength limit of natural fiber reinforced composites. The F_P value as the ending point of plastic zone used to calculate the MOR and plastic work (Fig. 1) and shows the maximum load capacity of composites before failure. The biodegradable

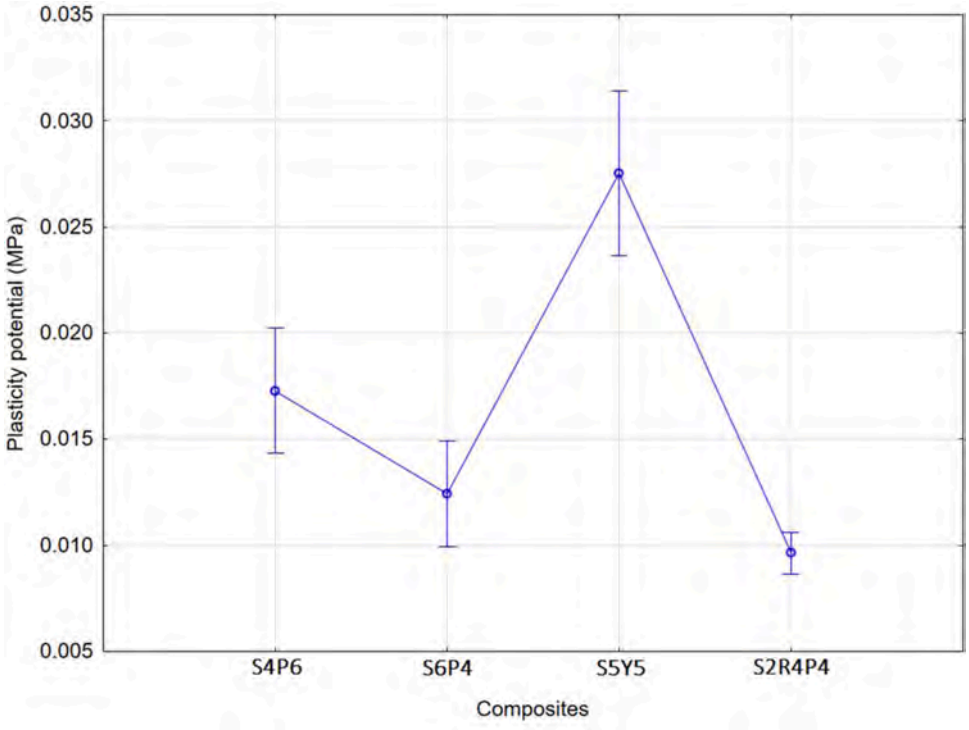

Fig. 9. The effect of different compositions on plasticity potential of composites.

Table 7
The Duncan's test results of the plasticity potential of reinforced composites as function of different composition.

Composites		(1) 0.01729	(2) 0.01242	(3) 0.02752	(4) 0.00964
1	S4P6		0.008235	0.000122	0.000187
2	S6P4	0.008235		0.000063	0.118478
3	S5Y5	0.000122	0.000063		0.000053
4	S2R4P4	0.000187	0.118478	0.000053	

Table 8
The effect of filling wood-plastic composites with wood dust and various types of polymers on their bending characteristics in the plastic range.

Composites	E_E (MPa)	E_{MV} (MPa)	E_P (MPa)	CH_M (MPa)
S4P6	1961	1010	866	670
S6P4	1389	631	528	394
S5Y5	4877	3244	2892	2345
S2R4P4	1391	562	480	378

filled composites with 50 % sawdust demonstrated higher force (471.095 N) between all studied composites. The effect of natural fiber to polymer ratio on maximum force at the strength limit was obvious from Fig. 10, where with increasing sawdust particles, the maximum force decreased up to 178.134 N and 130.181 N for reinforced composites containing 60 % sawdust and 60 % mixed fillers (sawdust/rubber), respectively. All reinforced composites showed significant difference in maximum force at strength limit which was verified by results of Duncan grouping test (Table 10). The noticeable reduction of maximum force by increasing sawdust particles from 40 to 60 % may be due to lower covering ability of polymer matrix in higher filler ratio of 60 % and more [26]. According to Fig. 10, the 40 % sawdust rPET composites depicted the best performance (251.969 N) among rPET bio-composites (Fig. 10).

The maximum deflection at the strength limit of composites illustrated higher deflection of rPET based composite compared to biodegradable reinforced composite (Fig. 11). Regarding the obtained results,

Table 9
The Duncan's test results of the bending modules of reinforced composites as function of different composition.

Duncan's test results of the tangent modulus at the proportionality limit (E_E)

Composites		(1) 1961.20	(2) 1388.50	(3) 4876.70	(4) 1391.50
1	S4P6		0.009577	0.000121	0.007491
2	S6P4	0.009577		0.000053	0.988431
3	S5Y5	0.000121	0.000053		0.000063
4	S2R4P4	0.007491	0.988431	0.000063	

Duncan's test results of the middle point's tangent modulus (E_{MV})

Composites		(1) 1010.20	(2) 630.65	(3) 3243.50	(4) 562.48
1	S4P6		0.010023	0.000121	0.003872
2	S6P4	0.010023		0.000063	0.627812
3	S5Y5	0.000121	0.000063		0.000063
4	S2R4P4	0.003872	0.627812	0.000063	

Duncan's test results of the MOR point's tangent modulus (E_P)

Composites		(1) 865.96	(2) 528.40	(3) 2892.00	(4) 479.88
1	S4P6		0.012407	0.000121	0.006419
2	S6P4	0.012407		0.000063	0.707093
3	S5Y5	0.000121	0.000063		0.000053
4	S2R4P4	0.006419	0.707093	0.000053	

Duncan's test results of the chord modulus (CH_M)

Composites		(1) 669.96	(2) 394.00	(3) 2345.20	(4) 377.92
1	S4P6		0.018228	0.000121	0.016889
2	S6P4	0.018228		0.000063	0.886192
3	S5Y5	0.000121	0.000063		0.000053
4	S2R4P4	0.016889	0.886192	0.000053	

the minimum deflection (7.002 mm) belongs to biodegradable composite containing 50 % sawdust and the maximum deflection at the strength limit (14.999 mm) observed for 60 % sawdust rPET composite. There was no significant difference between 40 % sawdust filled

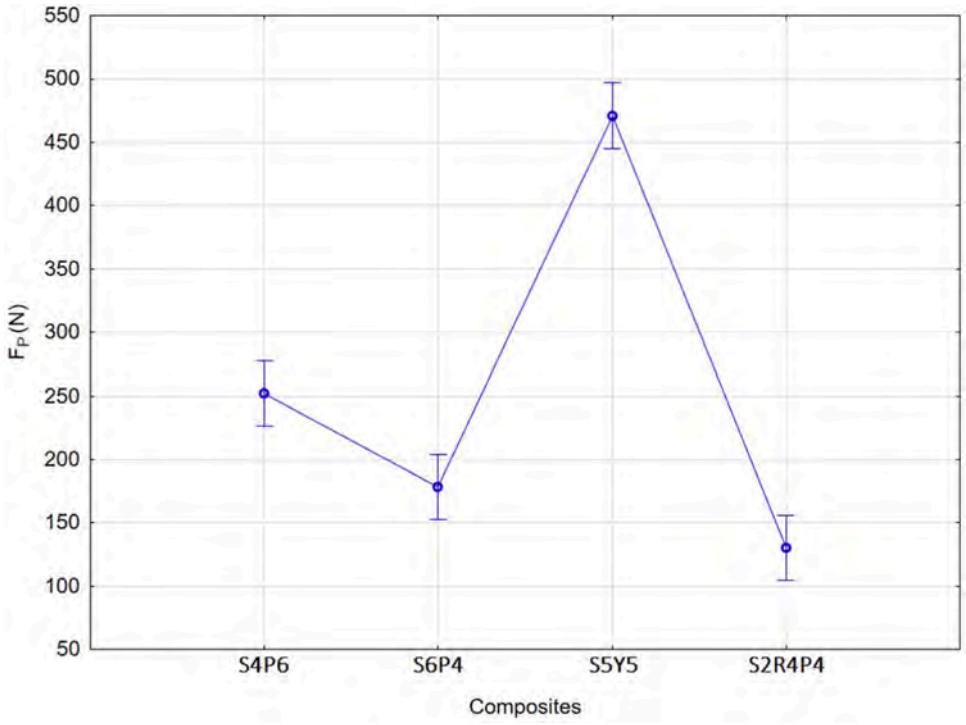

Fig. 10. The effect of different compositions on maximum force at the strength limit of composites.

Table 10
The Duncan's test results of the force at the strength limit of reinforced composites as function of different composition.

Composites		(1) 251.97	(2) 178.13	(3) 471.10	(4) 130.18
1	S4P6		0.000339	0.000121	0.000063
2	S6P4	0.000339		0.000063	0.011758
3	S5Y5	0.000121	0.000063		0.000053
4	S2R4P4	0.000063	0.011758	0.000053	

composite with 60 % mixed filled composite containing 40 % rubber and 20 % sawdust according to the Duncan test results (Table 11).

4. Numerical simulation

4.1. Model

Appropriate 3D models were prepared for numerical calculations (Fig. 12), taking into account each type of composite used. Solid models saved in Autodesk Inventor Professional 2022 (Autodesk Inc. San Francisco, California, USA) (*.stp) were imported into Abaqus v6.13–1 (Dassault Systems Simulia Corp. Providence, USA). The indenter and supports were made as rigid bodies in the shape of a half-cylinder with a diameter of 30 mm. Global hard contact interaction was used between the contacting surfaces of the beam, indenter, and support for normal behaviors. For tangential behavior, a friction coefficient of 0.1 was assumed [40–46]. An isotropic plastic damage model was also used, determined based on the stress-strain relationship for each tested composite (Fig. 13). According to the experimental results described above, the elastic properties of the materials are given in table 12. Since the supports and indenter were made as rigid bodies, elements of the R3D4 type (a 4-node 3-D bilinear rigid quadrilateral) were used (Fig. 12). For the modeling of the beams, the C3D8R elements (an 8-node linear brick, reduced integration, hourglass control) were used. The convergence of the numerical models was determined by repeated refinement of the beam mesh to a size of 2 mm, which ensured satisfactory agreement between the results of numerical calculations and laboratory measurements (Fig. 14). The parameter for removing elements if the stresses exceed the bending strength of materials (MOR) was also selected (Table 12). So, as the load increased, the elements reached a critical strain energy release rate, which led to failure and automatic removal of the elements. Appropriate boundary conditions for three-point bending were applied to both supports. A displacement ranging from 8 mm to 16 mm was imposed on the indenter, based on the experimental deflection amount. The calculations were performed at the Poznań Supercomputing and Networking Center (Poznań, Poland) using the Eagle computing cluster. where: D_e density (kg/m^3), E_E tangent modulus at the point of elasticity (MPa), ε_f fracture strain, $\dot{\varepsilon}^{pl}$ strain rate - the equivalent plastic strain rate, *MOR* modulus of rupture, η stress triaxiality, ν Poisson's ratio.

4.2. Results of numerical simulation

Fig. 14 compares the results of numerical calculations with the results of experimental studies. This figure shows that satisfactory convergence of the numerical models was achieved because the load-deflection curves of the numerical beams are well-matched to the curves illustrating the average values of the experimental results. Each numerical curve is within the range of maximum and minimum experimental values. Numerical models for composites S4P6, S6P4, and S2R4P4 also show the effect of beam destruction by cracking and a sharp drop in load values with deflections usually above 10 mm. These phenomena have also been confirmed experimentally. In the case of the S5Y5 composite, a maximum deflection of 8 mm was observed, corresponding to the experimental deflection, but without the effect of beam destruction. Since, in experimental tests, a sudden crack usually occurred after exceeding the deflection from 6.78 mm to 8.71 mm, it should be assumed that this phenomenon would also be observed for larger deflections in the numerical model.

Fig. 15 shows the distribution of normal stresses in the type S4P6 beam before and after its failure. Before failure, the maximum stresses in the beam reach 15.99 MPa (Fig. 15a). This value is 13.9 % lower than the experimental strength of 18.58 MPa. When this value is exceeded,

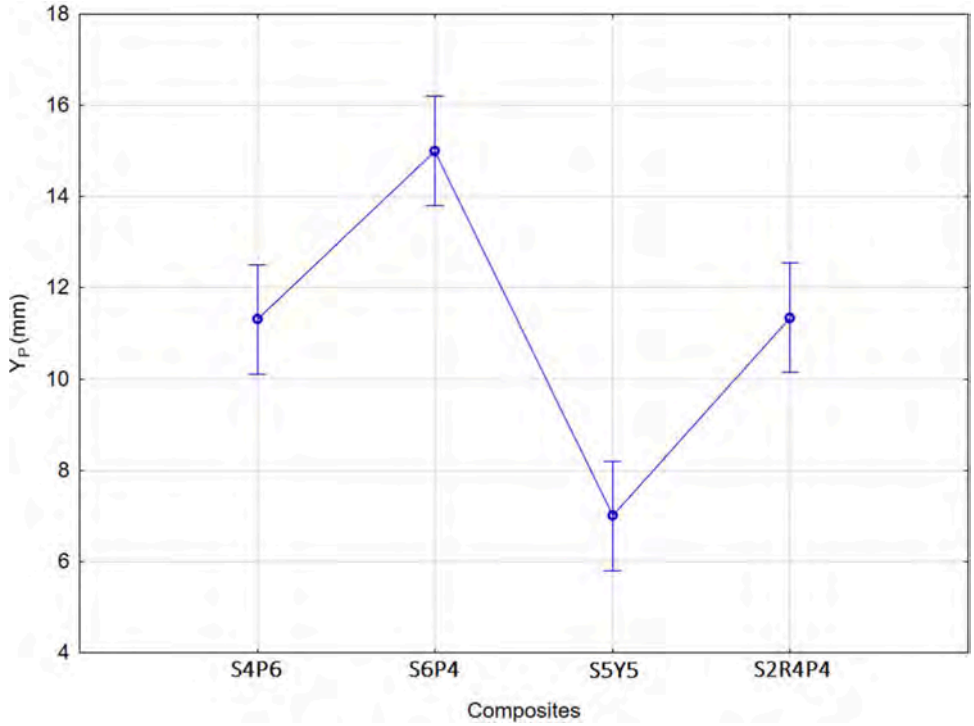

Fig. 11. The effect of different compositions on the maximum deflection at the strength limit of composites.

Table 11
The Duncan's test results of the maximum deflection at the strength limit of reinforced composites as function of different composition.

Composites		(1) 11.311	(2) 14.999	(3) 7.0027	(4) 11.342
1	S4P6		0.000189	0.000129	0.971220
2	S6P4	0.000189		0.000053	0.000218
3	S5Y5	0.000129	0.000053		0.000074
4	S2R4P4	0.971220	0.000218	0.000074	

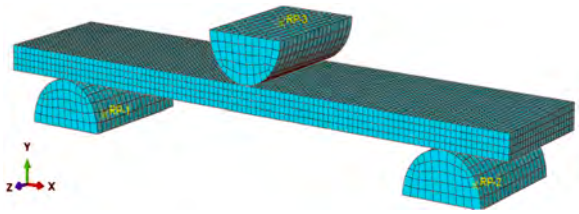

Fig. 12. FEM model of three-point bending test.

the beam cracks, and the stress in the damaged section decreases to 5.46 MPa (Fig. 15b). This figure shows that the crack appears both in the top and bottom surfaces of the beam, which indicates critical tensile and compressive stresses on the outer surfaces of the composite.

In the case of the S6P4 composite, the stresses that destroy the beam reach lower values compared to the S4P6 composite. Fig. 16a shows that before failure, the maximum stresses in the beam reach 11.50 MPa. This value is lower than the experimental strength of 12.16 MPa by only 5.43 %. After exceeding the maximum stresses, the beam cracks, and the stress in the damaged section decreases to 4.23 MPa (Fig. 16b). This figure shows that the middle part of the beam is not damaged, and material losses appear only on the top and bottom surfaces of the beam. This indicates critical tensile and compressive stresses on the outer surfaces of the composite and no crack propagation through the entire thickness of the beam.

Experimental studies (Fig. 14c) and numerical calculations have shown that composite S5Y5 has the highest stiffness and strength of all tested materials. From Fig. 17, it can be seen that the maximum normal stresses have a value of 37.8 MPa. Concerning the experimental strength of 43.88 MPa, these stresses are lower by 13.85 %. Therefore, no characteristic material damage due to cracking in the zone of tensile fibers was observed. It should be noted that the stresses in the central part of the beam were distributed evenly on both the compressed and tensile sides. The calculations show that this is the most advantageous solution from the structural point of view.

The S2R4P4 composites demonstrated, the stresses that destroy the beam reach the lowest values in comparison with the other composites. Fig. 18a shows that before failure, the maximum stresses in the beam reach 9.7 MPa. This value is lower than the experimental strength of 10.32 MPa by only 6.0 %. After exceeding the maximum stress, the beam cracks, and the stress decreases to 4.79 MPa (Fig. 18b). This figure shows that the middle and upper parts of the beam are not damaged, and material losses appear only on the lower surface of the beam. This indicates critical tensile stresses only on the bottom surface of the composite and no crack propagation through the entire thickness of the beam.

Table 13 contains the values of E_E, E_{MV}, E_P, CH_M, calculated for the numerical models and compares them with those corresponding to the experimental results. This table shows that for E_E, the differences between the numerical model and the experiment are within acceptable limits from 2.8 % to 20.5 %. RegardingE_{MV}, these differences range from −11.6 % to 14.1 %, where minus means that the experimental values are lower. However, these differences are entirely acceptable and confirm the good quality of the numerical model. The differences for E_P, have a similar feature. In this case, they range from −0.5 % to 28.3 %. The most significant differences appeared in CH_M (from 22.1 % to 66.7 %) and resulted mainly from the more asymptotic courses of the load-deflection curves, especially for composites S4P6, S6P4, and S2R4P4.

5. Conclusion

The effects of various additives and polymer materials on mechanical

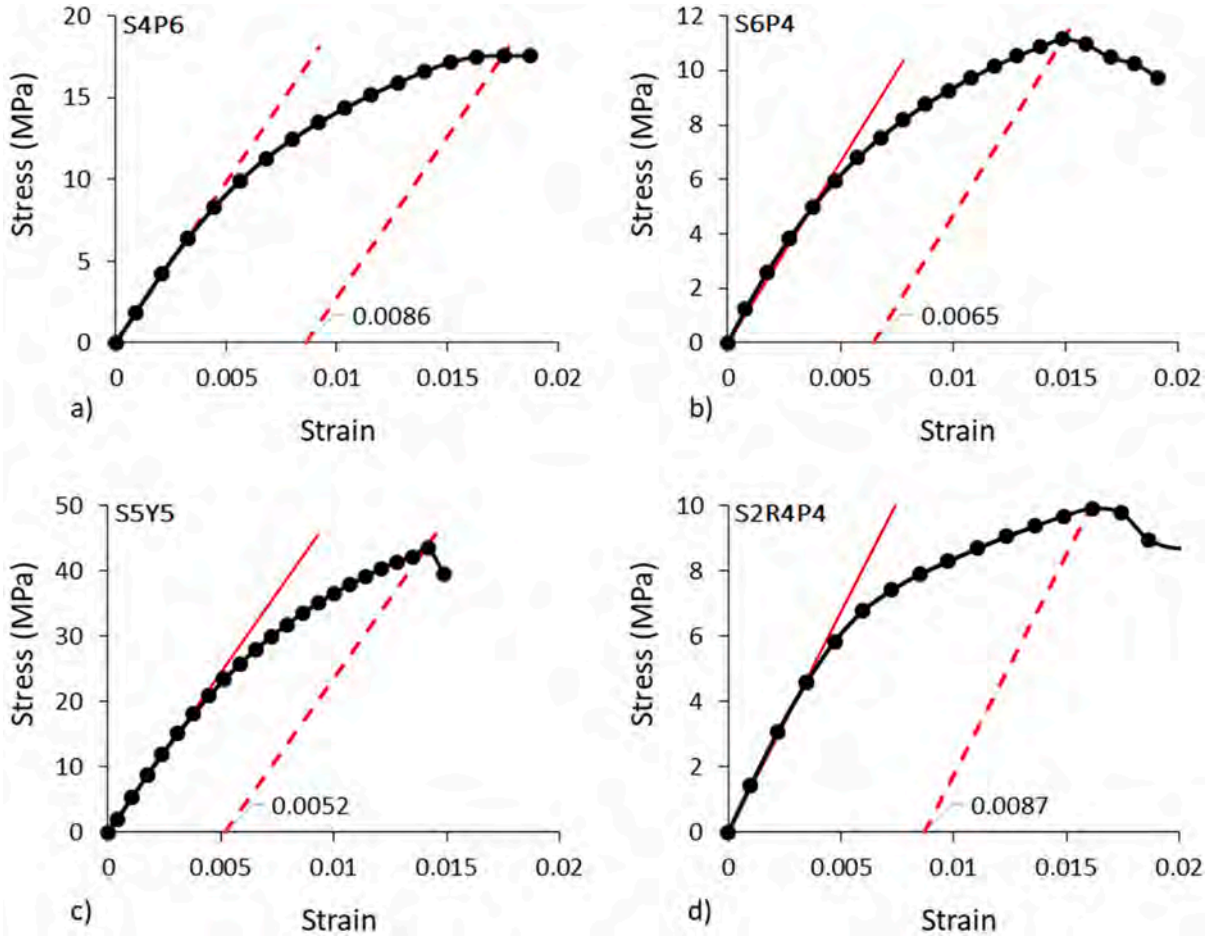

Fig. 13. Ductile damage model for composites: a) S4P6, b) S6P4, c) S5Y5, d) S2R4P4.

Table 12
The mechanical characteristics of composite materials.

Sample	E_E	*MOR*	ε_f	η	ε^{pl}	ν	D_e
	MPa						(kg/m^3)
S4P6	1961	18.58	0.0086	0.333	0.0017	0.3	941
S6P4	1389	12.16	0.0065	0.333	0.0017	0.3	909
S5Y5	4877	43.88	0.0052	0.333	0.0017	0.3	1190
S2R4P4	1391	10.32	0.0087	0.333	0.0017	0.3	1057

characteristics in the plastic range of a three-point bending test were evaluated in this study. The findings demonstrated that the mechanical properties of composites are influenced by both the filler and the matrix, while the matrix's influence being far more significant than the filler's amount and composition. The results indicated that the best mechanical characteristics was demonstrated by a biodegradable reinforced polymer containing 50 % sawdust, and Y1000P demonstrated superior mechanical properties compared to rPET polymer. The investigated results also revealed that the composite made with 40 % natural fibers showed greater mechanical properties compared to other rPET composites, and increasing filler content from 40 to 60 % led to a noticeable decrease in the mechanical properties of rPET-reinforced composites. The Duncan test showed no significant difference in the mechanical properties of 40 % rPET composites containing 60 % sawdust as well as mixed sawdust (20 %) and rubber particles (40 %). However, the biodegradable composites containing 50 % sawdust as well as 40 % sawdust-filled rPET composites met the ANSI standard requirements for medium-density fiberboard (MDF), and they could be introduced as an appropriate replacement for MDF in interior applications. Further research on the mechanical characteristics of bio-composites, especially in the plastic range, is therefore desirable with different filler materials, polymer matrixes, and also other additives such as coupling agents to improve interaction rPET-sawdust by decreasing the rPET's melting temperature. The presented favorable results of numerical calculations and their good fit to experimental values prove the correctness of the developed FEM models and the possibility of their practical application in modeling other similar wood-polymer composites.

Funding

The authors state no funding involved.

CRediT authorship contribution statement

S. Behnam Hosseini: Writing – original draft, Formal analysis. **Milan Gaff:** Supervision, Methodology. **Jerzy Smardzewski:** Supervision, Formal analysis.

Declaration of competing interest

The authors declare that they have no known competing financial interests or personal relationships that could have appeared to influence the work reported in this paper.

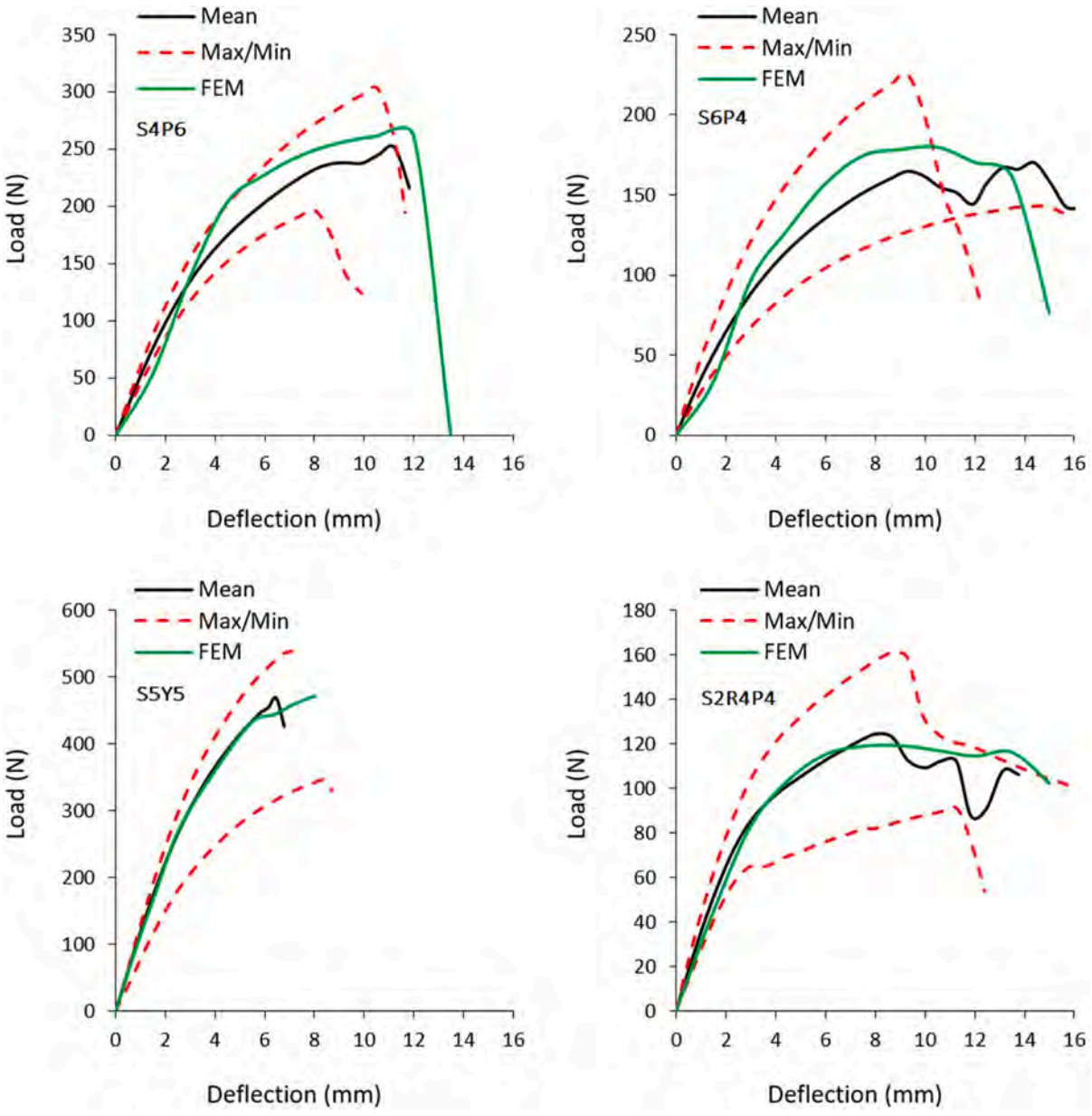

Fig. 14. Comparison experimental and FEM model of load-deflection relations: a) S4P6, b) S6P4, c) S5Y5, d) S2R4P4.

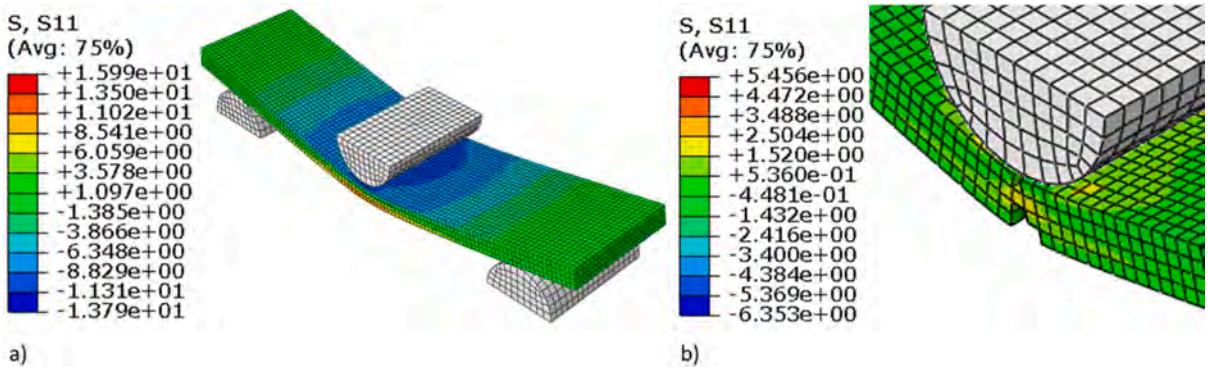

Fig. 15. Normal stress of composite S4P6: a) before and b) after break.

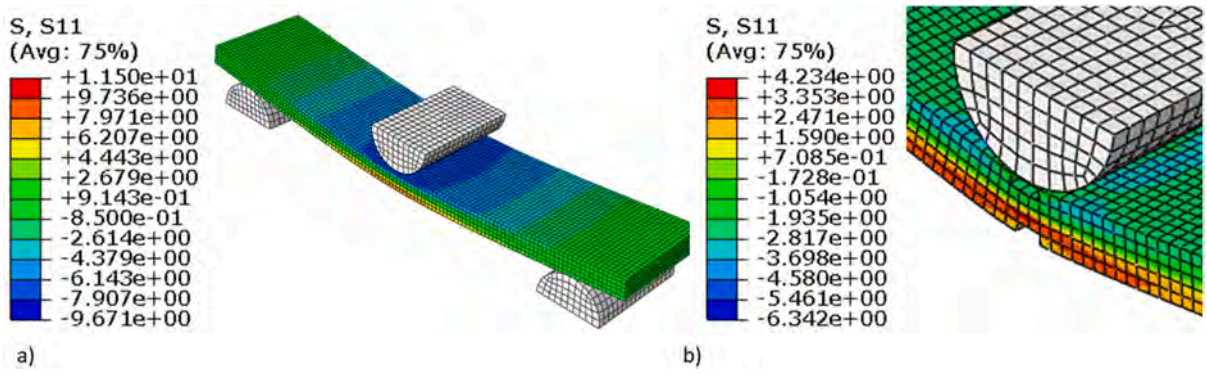

Fig. 16. Normal stress of composite S6P4: a) before and b) after break.

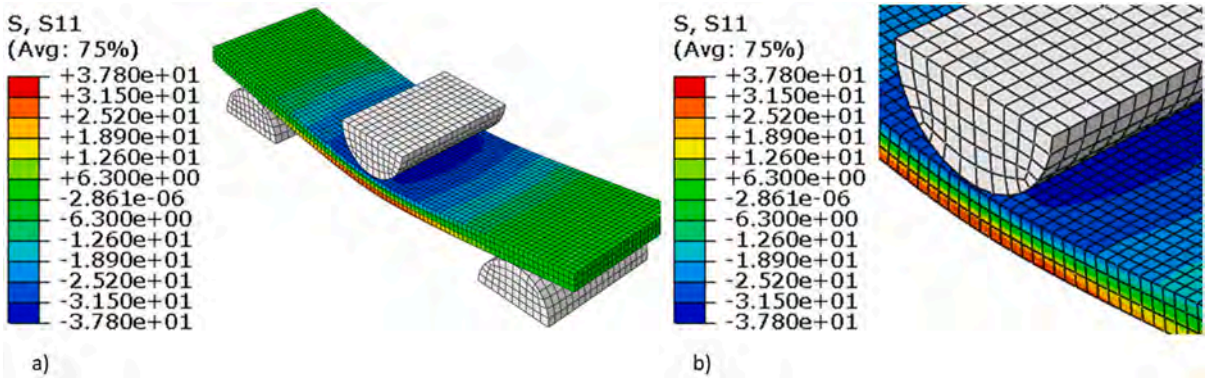

Fig. 17. Normal stress of composite S5Y5: a) before and b) after break.

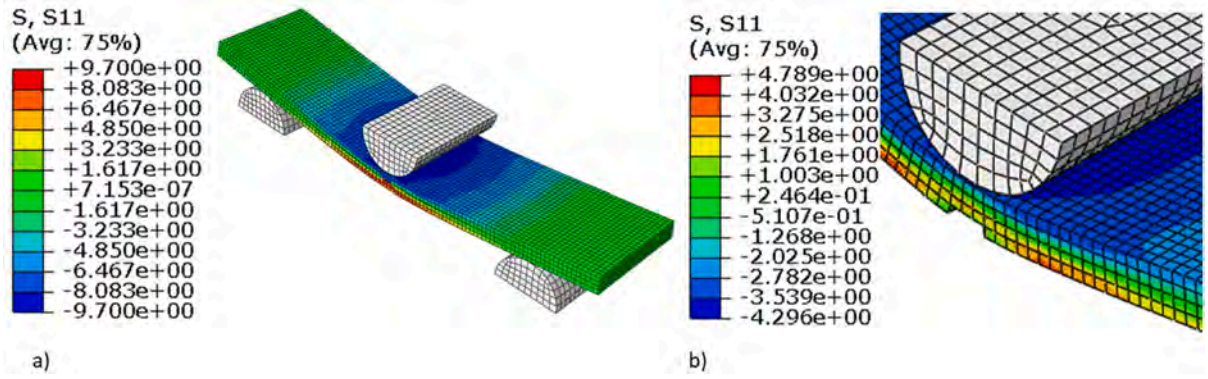

Fig. 18. Normal stress of composite S2R4P4: a) before and b) after break.

Table 13
Comparison of numerical and experimental results of sawdust reinforced composites.

Composites	Results	E_E (MPa)	E_{MV} (MPa)	E_P (MPa)	CH_M (MPa)
S4P6	Experiment	1961	1010	866	670
	FEM	1808	1127	871	309
	Difference (%)	7.8	−11.6	−0.5	53.9
S6P4	Experiment	1389	631	528	394
	FEM	1220	687	510	155
	Difference (%)	12.2	−8.9	3.4	60.6
S5Y5	Experiment	4877	3244	2892	2345
	FEM	4740	3282	2797	1826
	Difference (%)	2.8	−1.2	3.3	22.1
S2R4P4	Experiment	1391	562	480	378
	FEM	1106	483	344	126
	Difference (%)	20.5	14.1	28.3	66.7

Acknowledgements

The authors would like to thank the Department of Furniture, Design and Habitat Brno, Mendel University in Brno and the Poznań Supercomputing and Networking Center (Poznań, Poland) for the close collaboration in this article. The study was extracted from results of Hosseini's PhD thesis and research.

Data availability

Data will be made available on request.

References

[1] H. Ku, H. Wang, N. Pattarachaiyakoop, M. Trada, A review on the tensile properties of natural fiber reinforced polymer composites, Engineering 42 (4) (2011) 856–873.
[2] M.J. Schwarzkopf, M.D. Burnard, Wood-plastic composites—Performance and environmental impacts, Environ. Impacts Trad. Innov. For.Based Bioproducts (2016) 19–43.
[3] F.P. La Mantia, M Morreale, Green composites: a brief review, Appl. Sci. Manufact. 42 (6) (2011) 579–588.
[4] S.B. Hosseini, M. Gaff, H. Li, D. Hui, Effect of fiber treatment on physical and mechanical properties of natural fiber-reinforced composites: a review, Rev. Adv. Mater. Sci. 62 (1) (2023) 20230131.
[5] S.B. Hosseini, S. Hedjazi, L. Jamalirad, A. Sukhtesaraie, Effect of nano-SiO 2 on physical and mechanical properties of fiber reinforced composites (FRCs), J. Ind. Acade. Wood Sci. 11 (2014) 116–121.
[6] S.B. Hosseini, Effects of Dioctyl phthalate and density changes on the physical and mechanical properties of woodflour/PVC composites, J. Indian Acad. Wood Sci. 10 (2013) 22–25.
[7] J.M. Felix, P. Gatenholm, The nature of adhesion in composites of modified cellulose fibers and polypropylene, J. Appl. Polym. Sci. 42 (3) (1991) 609–620.
[8] K. Joseph, S. Thomas, C. Pavithran, Effect of chemical treatment on the tensile properties of short sisal fibre-reinforced polyethylene composites, Polymer. (Guildf) 37 (23) (1996) 5139–5149.
[9] A.K. Bledzki, S. Reihmane, J. Gassan, Properties and modification methods for vegetable fibers for natural fiber composites, J. Appl. Polym. Sci. 59 (8) (1996) 1329–1336.
[10] J. Gassan, A.K. Bledzki, The influence of fiber-surface treatment on the mechanical properties of jute-polypropylene composites, Appl. Sci. Manufact. 28 (12) (1997) 1001–1005.
[11] H.D. Rozman, G.S. Tay, R.N. Kumar, A. Abubakar, H. Ismail, Z.M. Ishak, Polypropylene hybrid composites: a preliminary study on the use of glass and coconut fiber as reinforcements in polypropylene composites, Polym. Plast. Technol. Eng. 38 (5) (1999) 997–1011.
[12] H.D. Rozman, G.S. Tay, R.N. Kumar, A. Abusamah, H. Ismail, Z.M. Ishak, Polypropylene–oil palm empty fruit bunch–glass fibre hybrid composites: a preliminary study on the flexural and tensile properties, Eur. Polym. J. 37 (6) (2001) 1283–1291.
[13] H.D. Rozman, B.K. Kon, A. Abusamah, R.N. Kumar, Z.M. Ishak, Rubberwood–high-density polyethylene composites: effect of filler size and coupling agents on mechanical properties, J. Appl. Polym. Sci. 69 (10) (1998) 1993–2004.
[14] A. Valadez-Gonzalez, J.M. Cervantes-Uc, R.J.I.P. Olayo, P.J. Herrera-Franco, Effect of fiber surface treatment on the fiber–matrix bond strength of natural fiber reinforced composites, Engineering 30 (3) (1999) 309–320.
[15] N.E. Marcovich, M.M. Reboredo, M.I. Aranguren, Mechanical properties of woodflour unsaturated polyester composites, J. Appl. Polym. Sci. 70 (11) (1998) 2121–2131.
[16] J. Gassan, A study of fibre and interface parameters affecting the fatigue behaviour of natural fibre composites, Appl. Sci. Manufact. 33 (3) (2002) 369–374.
[17] N.E. Marcovich, M.I. Aranguren, M.M. Reboredo, Modified woodflour as thermoset fillersPart I. Effect of the chemical modification and percentage of filler on the mechanical properties, Polymer. (Guildf) 42 (2) (2001) 815–825.
[18] N.E. Marcovich, M.M. Reboredo, M.I. Aranguren, Modified woodflour as thermoset fillers: II. Thermal degradation of woodflours and composites, Thermochim. Acta 372 (1–2) (2001) 45–57.
[19] M. Babiak, M. Gaff, A. Sikora, Š. Hysek, Modulus of elasticity in three-and four-point bending of wood, Compos. Struct. 204 (2018) 454–465.
[20] M. Gaff, M. Babiak, Tangent modulus as a function of selected factors, Compos. Struct. 202 (2018) 436–446.
[21] A. Požgaj, D. Chovanec, S. Kurjatko, M. Babiak, Štruktúra a Vlastnosti Dreva, Príroda, 1993.
[22] M. Gaff, M. Gašparík, M. Babiak, V. Vokatý, Bendability characteristics of wood lamellae in plastic region, Compos. Struct. 163 (2017) 410–422.
[23] K.S. Rahman, M.N. Islam, M.M. Rahman, M.O. Hannan, R. Dungani, H.A. Khalil, Flat-pressed wood plastic composites from sawdust and recycled polyethylene terephthalate (PET): physical and mechanical properties, Springerplus. 2 (2013) 1–7.
[24] V. Jost, H.C. Langowski, Effect of different plasticisers on the mechanical and barrier properties of extruded cast PHBV films, Eur. Polym. J. 68 (2015) 302–312.
[25] G. Janowski, W. Frącz, Ł. Bąk, The Mechanical properties prediction of poly [(3-hydroxybutyrate)-co-(3-hydroxyvalerate)](PHBV) biocomposites on a chosen example, Materials. 15 (21) (2022) 7531.
[26] H.C. Chen, T.Y. Chen, C.H. Hsu, Effects of wood particle size and mixing ratios of HDPE on the properties of the composites, Euro. J. Wood Wood Products 64 (3) (2006) 172–177.
[27] A. Sikora, M. Gaff, Š. Hysek, M. Babiak, The plasticity of composite material based on winter rapeseed as a function of selected factors, Compos. Struct. 202 (2018) 783–792.
[28] A.R. Sanadi, J.F. Hunt, D.F. Caulfield, G. Kovacsvolgyi, B. Destree, High fiber-low matrix composites: kenaf fiber/polypropylene, in: Proceedings of 6th international conference on woodfiber-plastic composites, 2001, pp. 15–16.
[29] R.G. Raj, B.V. Kokta, D. Maldas, C. Daneault, Use of wood fibers in thermoplastics. VII. The effect of coupling agents in polyethylene–wood fiber composites, J. Appl. Polym. Sci. 37 (4) (1989) 1089–1103.
[30] M. Chaharmahali, J. Mirbagheri, M. Tajvidi, S.K. Najafi, Y. Mirbagheri, Mechanical and physical properties of wood-plastic composite panels, J. Reinf. Plast. Compos. 29 (2) (2010) 310–319.
[31] N. Ayrilmis, S. Jarusombuti, Flat-pressed wood plastic composite as an alternative to conventional wood-based panels, J. Compos. Mater. 45 (1) (2011) 103–112.
[32] P. Klímek, T. Morávek, J. Ráhel, M. Stupavská, D. Děcký, P. Král, R. Wimmer, Utilization of air-plasma treated waste polyethylene terephthalate particles as a raw material for particleboard production, Engineering 90 (2016) 188–194.
[33] T.M. Maloney, Modern particleboard and dry-process fiberboard manufacturing, 1977, p. 672. -pp.
[34] M.A. Berthet, H. Angellier-Coussy, V. Chea, V. Guillard, E. Gastaldi, N. Gontard, Sustainable food packaging: valorising wheat straw fibres for tuning PHBV-based composites properties, Appl. Sci. Manufact. 72 (2015) 139–147.
[35] R.M. Allaf, E. Albarahmieh, M. Futian, Preparation of sawdust-filled recycled-PET composites via solid-state compounding, Processes 8 (1) (2020) 100.
[36] D. Ndiaye, B. Diop, C. Thiandoume, P.A. Fall, A.K. Farota, A. Tidjani, Morphology and thermo mechanical properties of wood/polypropylene composites, Polypropylene, 4 (2012) 415–428.
[37] J.Z. Lu, Q. Wu, I.I. Negulescu, Wood-fiber/high-density-polyethylene composites: coupling agent performance, J. Appl. Polym. Sci. 96 (1) (2005) 93–102.
[38] W. Wang, Y. Peng, Y. Dong, K. Wang, J. Li, W. Zhang, Effect of coupling agent modified intumescent flame retardant on the mechanical properties, thermal degradation behavior, and flame retardancy of wood-flour/polypropylene composites, Polym. Compos. 39 (3) (2018) 826–834.
[39] F.M. Coutinho, T.H. Costa, D.L. Carvalho, Polypropylene–wood fiber composites: effect of treatment and mixing conditions on mechanical properties, J. Appl. Polym. Sci. 65 (6) (1997) 1227–1235.
[40] J. Smardzewski, K.W. Wojciechowski, Study on the bending and failure behaviour of wooden sandwich panels with corrugated core, randomized gaps, and wood defects, Constr. Build. Mater. 409 (2023) 133924.
[41] A. Ingrole, A. Hao, R. Liang, Design and modeling of auxetic and hybrid honeycomb structures for in-plane property enhancement, Mater. Des. 117 (2017) 72–83.
[42] X. Li, Z. Lu, Z. Yang, Q. Wang, Y. Zhang, Yield surfaces of periodic honeycombs with tunable Poisson's ratio, Int. J. Mech. Sci. 141 (2018) 290–302.
[43] L.L. Hu, Z.R. Luo, Q.Y. Yin, Negative Poisson's ratio effect of re-entrant anti-trichiral honeycombs under large deformation, Thin-Walled Struct. 141 (2019) 283–292.
[44] P. Chen, H. Wu, W. Zhu, L. Yang, Z. Li, C. Yan, Y. Shi, Investigation into the processability, recyclability and crystalline structure of selective laser sintered Polyamide 6 in comparison with Polyamide 12, Polym. Test. 69 (2018) 366–374.
[45] Y. Sha, L. Jiani, C. Haoyu, R.O. Ritchie, X. Jun, Design and strengthening mechanisms in hierarchical architected materials processed using additive manufacturing, Int. J. Mech. Sci. 149 (2018) 150–163.
[46] X. Li, Z. Lu, Z. Yang, C. Yang, Anisotropic in-plane mechanical behavior of square honeycombs under off-axis loading, Mater. Des. 158 (2018) 88–97.